

Supporting Information for

Competitive Lithium Solvation of Linear and Cyclic Carbonates from Quantum Chemistry

O. Borodin,^{a,*} M. Olguin,^a P. Ganesh,^b P. R. C. Kent,^{b,c} Joshua L. Allen^a, Wesley A. Henderson^d

^a Electrochemistry Branch, RDRL-SED-C, Powder Mill Rd. 2800, US Army Research Laboratory, Adelphi, MD, 20783-1138, USA

^b Center for Nanophase Materials Sciences, Oak Ridge National Laboratory, 1 Bethel Valley Road, Oak Ridge, TN 37831, USA

^c Computer Science and Mathematics Division, Oak Ridge National Laboratory, 1 Bethel Valley Road, Oak Ridge, TN 37831, USA

^d Electrochemical Materials & Systems Group, Energy & Environment Directorate, Pacific Northwest National Laboratory (PNNL), Richland, Washington 99352, USA

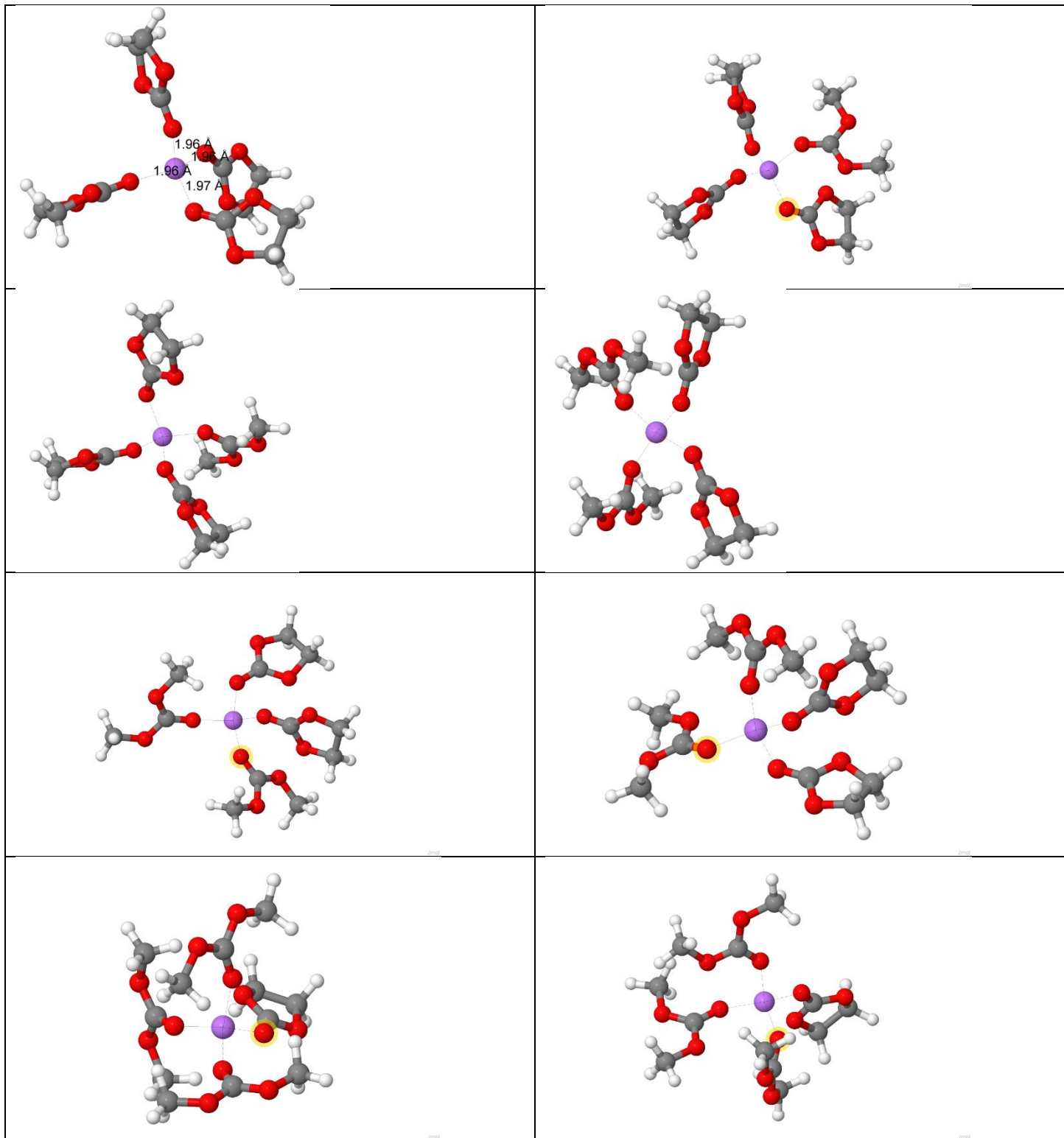
More Detailed Description of BOMB Simulations using CP2K Software

Born-Oppenheimer Molecular Dynamics Simulations of EC:DMC/LiPF₆ Electrolytes. BOMB simulations were also performed for EC:DMC(1:1 mol%)/LiPF₆ at two additional salt concentrations: low salt concentration (LC) (EC)₁₅:(DMC)₁₅:(LiPF₆)₃ and high salt concentration (HC) (EC)₁₆:(DMC)₁₆:(LiPF₆)₉ at 393 K. BOMB simulations were performed using a hybrid Gaussian and Plane Wave (GPW) density functional scheme as implemented in the CP2K/QUICKSTEP program. Central to the GPW method is a dual representation combining a basis of atom centred Gaussian orbitals to describe the system wavefunction and an auxiliary plane wave basis set to describe the electronic density. The compact representation of the wavefunction in the GPW method allows for the Kohn-Sham matrix to be constructed in near linear scaling time. The orbital transformation (OT) method implemented in CP2K/QUICKSTEP is a direct energy functional minimization scheme that allows for a fast (significantly faster than diagonalization/DIIS based methods) and efficient wavefunction optimization guaranteed to converge. Ab initio molecular dynamics simulations based on the Born-Oppenheimer approach can be performed efficiently using a density matrix extrapolation scheme which directly provides a good initial trial wave function for each SCF calculation (as required for the OT method) using a multi-linear extrapolation of energy-minimized wavefunctions from previous trajectory steps.

The GPW approach makes use of pseudopotentials (PP) to represent core electrons, where the PPs used for the present study are of the analytical dual-space Goedecker-Teter-Hutter (GTH) type including relativistic core corrections in combination with the spin-polarized PBE functional formulation of the generalized gradient approximation. Contracted gaussian basis sets (denoted as MOLOPT), where the exponents and contraction coefficients were obtained by minimizing a linear combination of the total energy and the condition number of the overlap matrix for a set of molecules, were used to describe valence electrons for all atoms. The MOLOPT basis sets exhibit no near linear dependencies in the basis, ensuring that the overlap matrix is always well conditioned, including in condensed phase systems, making the MOLOPT basis well suited to be used in first principles molecular dynamics simulations of electrolyte mixtures. Elements of the Kohn-Sham and overlap matrix smaller than $\epsilon_{\text{threshold}} \approx 10^{-12}$ were neglected.

Initial electrolyte configurations for the BOMB simulations were taken from MD simulations using the APPLE&P polarizable force field. Both LC and HC salt concentrations were simulated using the PBE functional in the isobaric-isothermal ensemble (NPT) at 1 bar with periodic boundary conditions applied to all three dimensions. For NPT simulations, the convergence of the pressure may require a significantly larger basis than the basis set required to obtain convergent properties for its constant volume (NVT) counterpart. In regard to the role of plane wave cutoff in the GPW method, previous work using the CP2K/QUICKSTEP code for an extensive set of variable-cell NPT simulations showed that the effect of the plane wave cutoff beyond 600 Ry and that the particular method for constructing the grids used in the numerical integration of the exchange-correlation and Hartree potential do not significantly influence the resulting density and structure of several condensed phase systems.¹ Thus, we employed a 500 Ry density grid for all NPT simulations. The Nose-Hoover thermostat was applied to all degrees of freedom using a time constant of 1 ps in conjunction with a barostat time constant of 1 ps. The nuclear equations of motion have been integrated using Tuckerman approach based on the Martyna-Tobias-Klein (MTK) algorithm² with a 1.0 fs time step and hydrogen masses.

A total of 20 picoseconds (ps) of NPT simulation time was obtained for the LC system and 38 ps for the HC mixture. Since the energy (energy vs. time) exhibited changes over the first 4 ps of the NPT simulation run, the first 4 ps of the simulation trajectory were discarded with the remaining trajectory used for analysis unless otherwise noted. The differences between the radial distribution functions (RDFs) from the first and second parts of MD trajectories are shown below in SI. In order to examine the influence of adding an empirical dispersion to the PBE functional on the Li⁺ solvation shell composition, a separate set of BOMB simulations were performed for LC electrolyte in the NVT ensemble using the electrolyte density obtained from classical MD simulations using the APPLE&P polarizable force field.



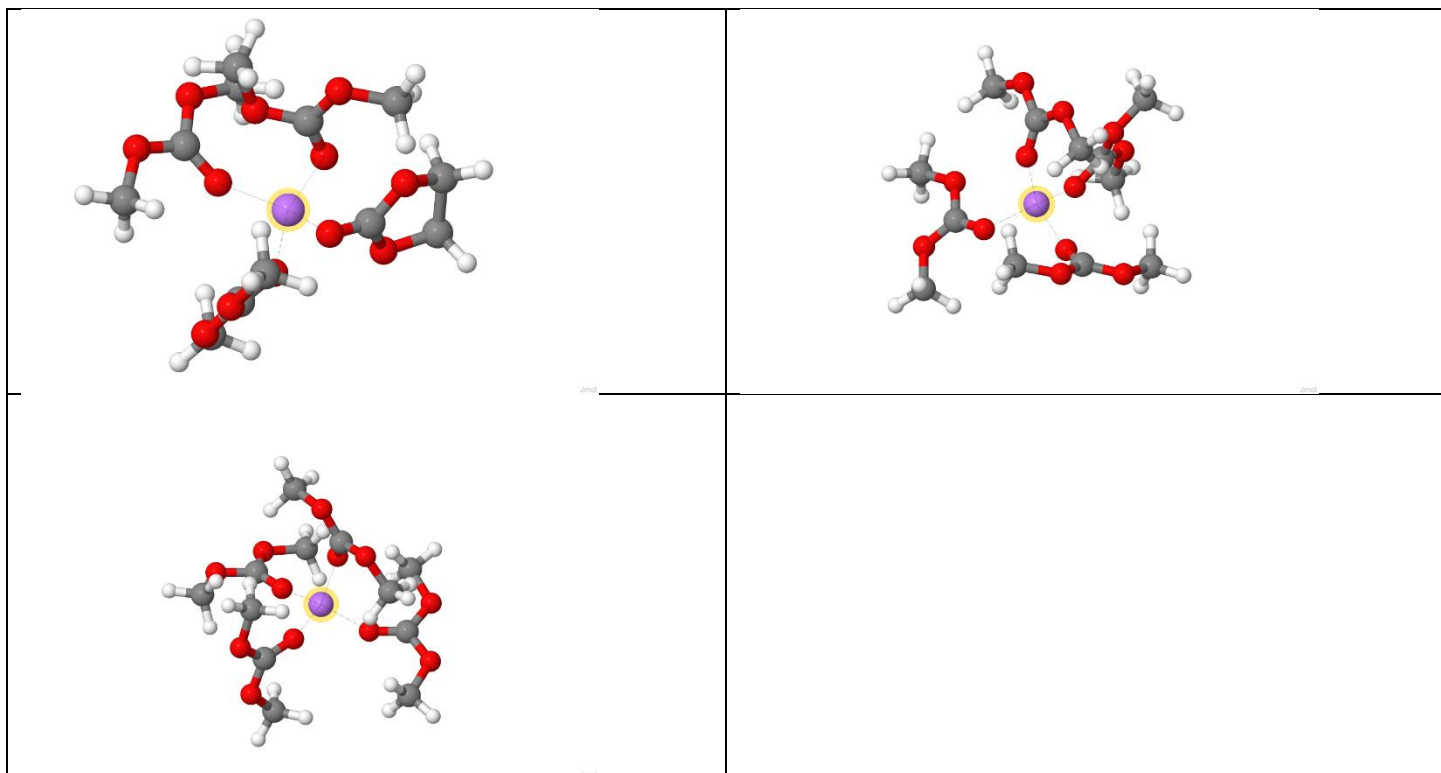


Fig. S1. Optimized geometries of $\text{Li}^+\text{EC}_n\text{DMC}_m$ clusters from PBE/6-31+G(d,p) calculations with SMD($\epsilon=20$, acetone)

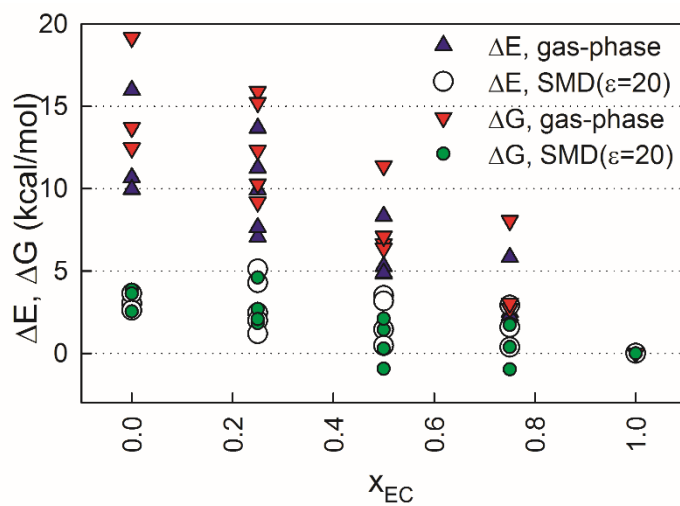


Fig.S2 The relative cluster binding energies from PBE/6-31+G(d,p) calculations with SMD($\epsilon=20$) and in gas-phase ($\epsilon=1$) for $(\text{EC})_n(\text{DMC})_m\text{-Li}^+$, $n+m=4$.

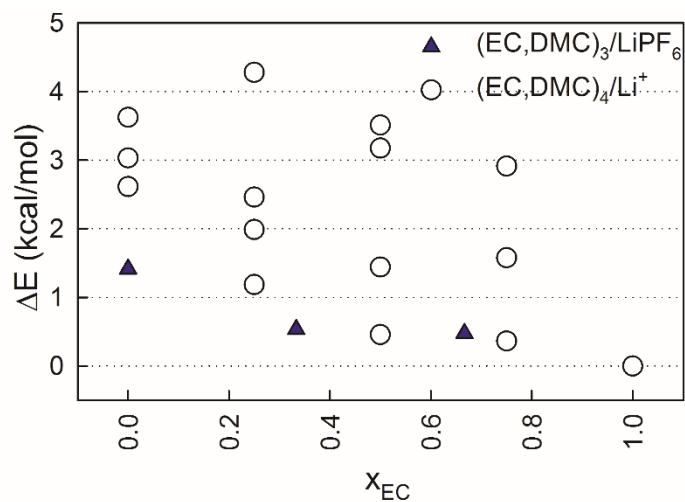


Fig. S3. Binding energies (ΔE) for (EC)_n(DMC)_m-Li⁺ solvates ($n+m=4$) relative to (EC)₄-Li⁺ and (EC)₃-LiPF₆ solvates from PBE/6-31+G(d,p), SMD($\epsilon=20$) calculations.

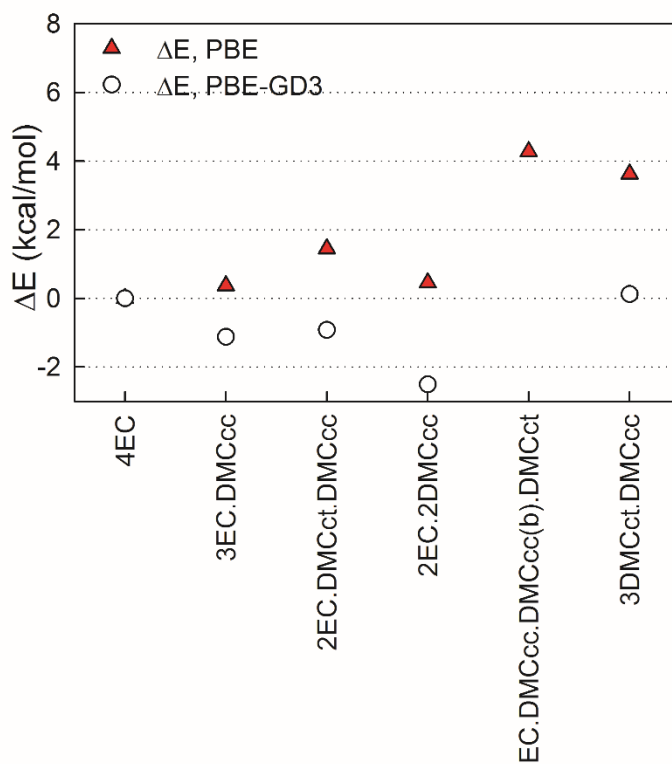


Fig. S4. Binding energies (ΔE) relative to (EC)₄-Li⁺ for selected (EC)_n(DMC)_m-Li⁺ solvates ($n+m=4$) from PBE and PBE-GD3 calculations with 6-31+G(d,p) basis set and SMD($\epsilon=20$) solvation model.

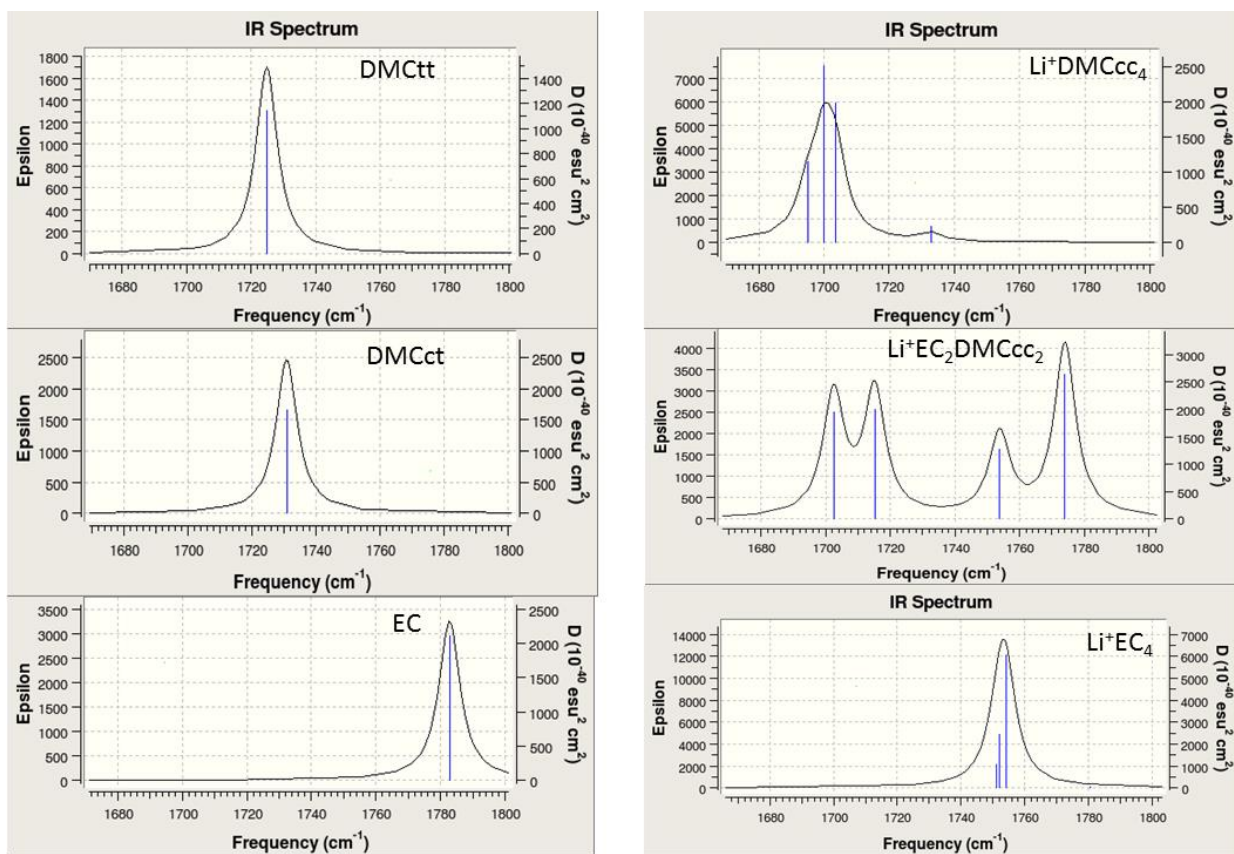


Fig. S5. IR spectrum of isolated DMC and EC and three Li⁺ solvates from PBE/6-31+G(d,p) with SMD($\epsilon=20$,acetone) calculations.

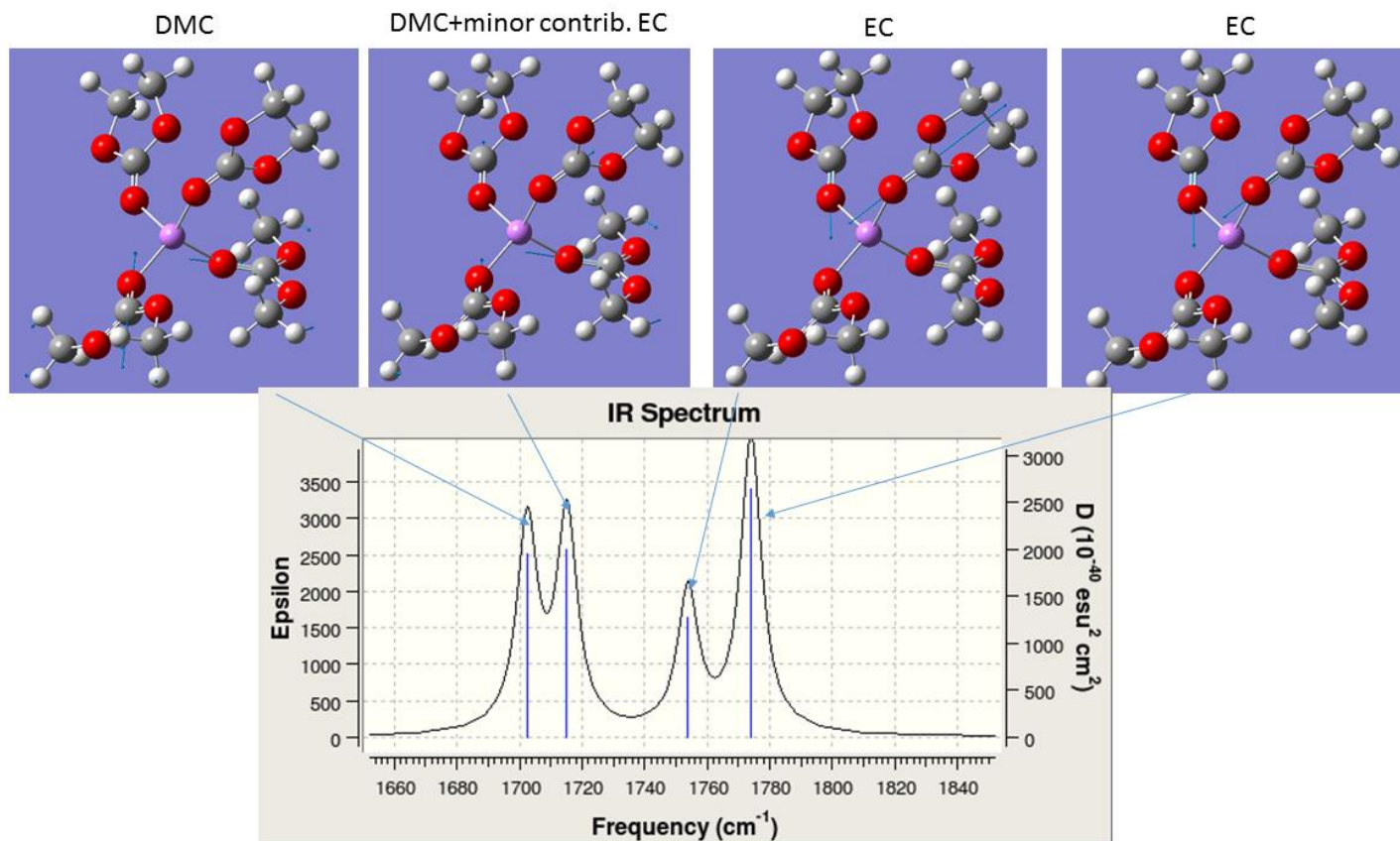


Fig. S6. Eigenvectors corresponding to vibrational band frequencies for $(EC)_2(DMC)_2-Li^+$ complex from PBE/6-31+G(d,p) calculations with SMD($\epsilon=20$, acetone).

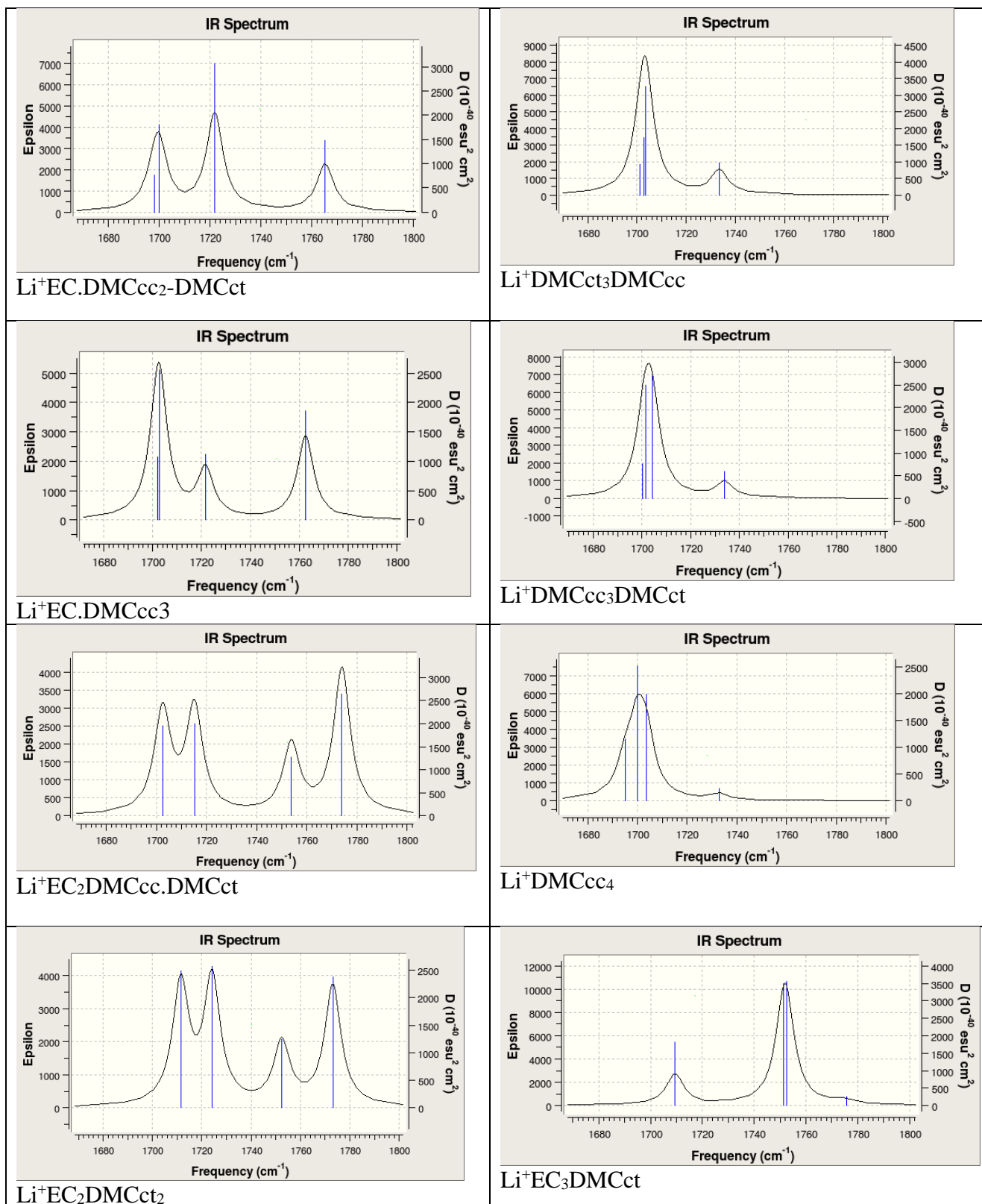


Fig. S7. IR spectrum of the C=O band from PBE/6-31+G** SMD($\epsilon=20$) calculations

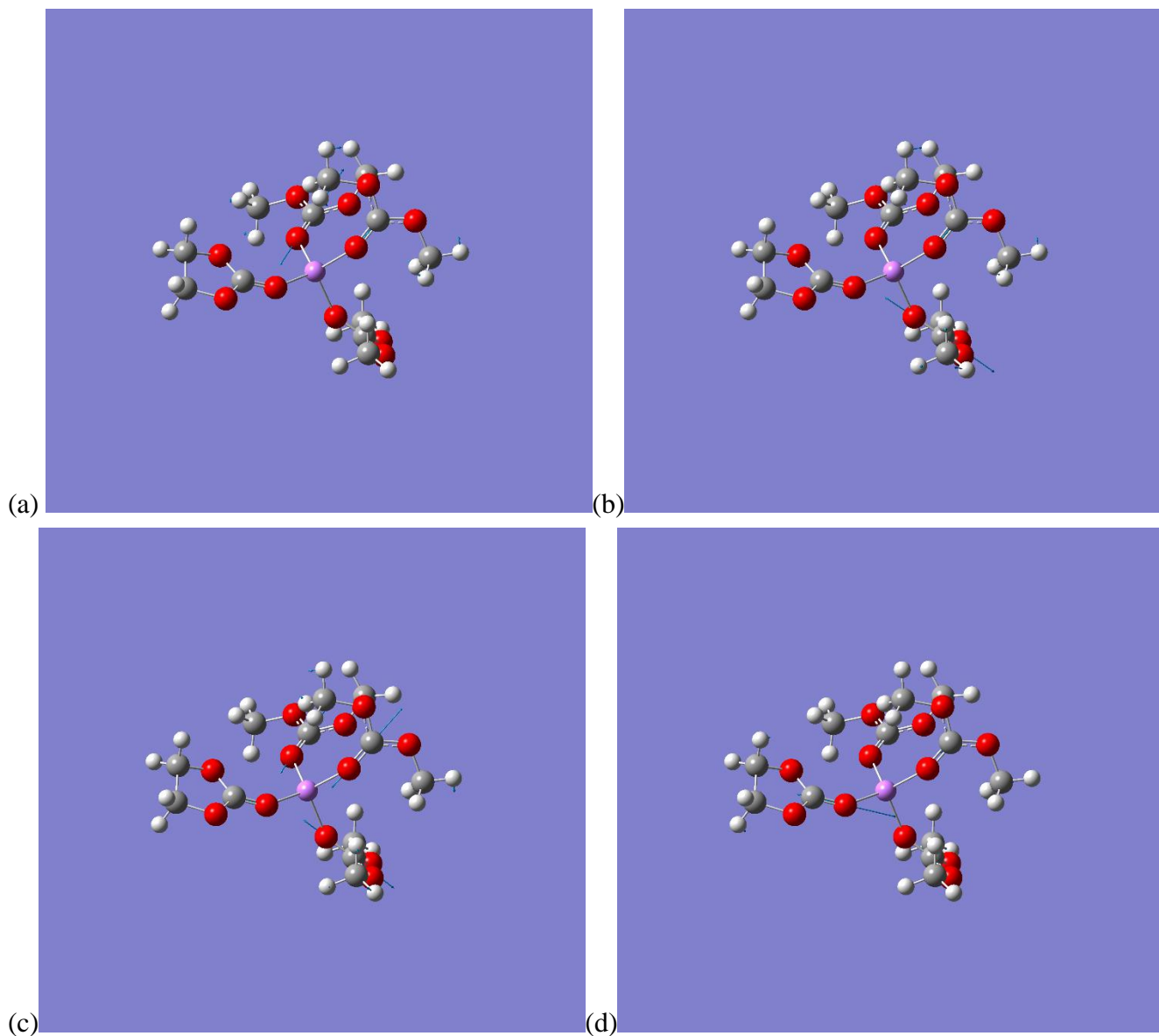


Fig. S8. Eigenvectors corresponding to vibrational band frequencies at 1869 (a), 1700 (b), 1722 (c) and 1765 cm^{-1} (d) from PBE/6-31+G(d,p) with SMD($\epsilon=20$, acetone) calculations of $(\text{EC})(\text{DMCcc})_2(\text{DMCct})\text{-Li}^+$. It shows that vibrational frequency of DMCct and DMCcc complex to a Li^+ cation are similar shown in (a) and (b) are similar, while vibrational frequency of DMCcc complex to a Li^+ could be effected by the environment (compare geom. b and c). Vibrational frequency of 1765 cm^{-1} corresponding to EC complexed to a Li^+ is the lowest.

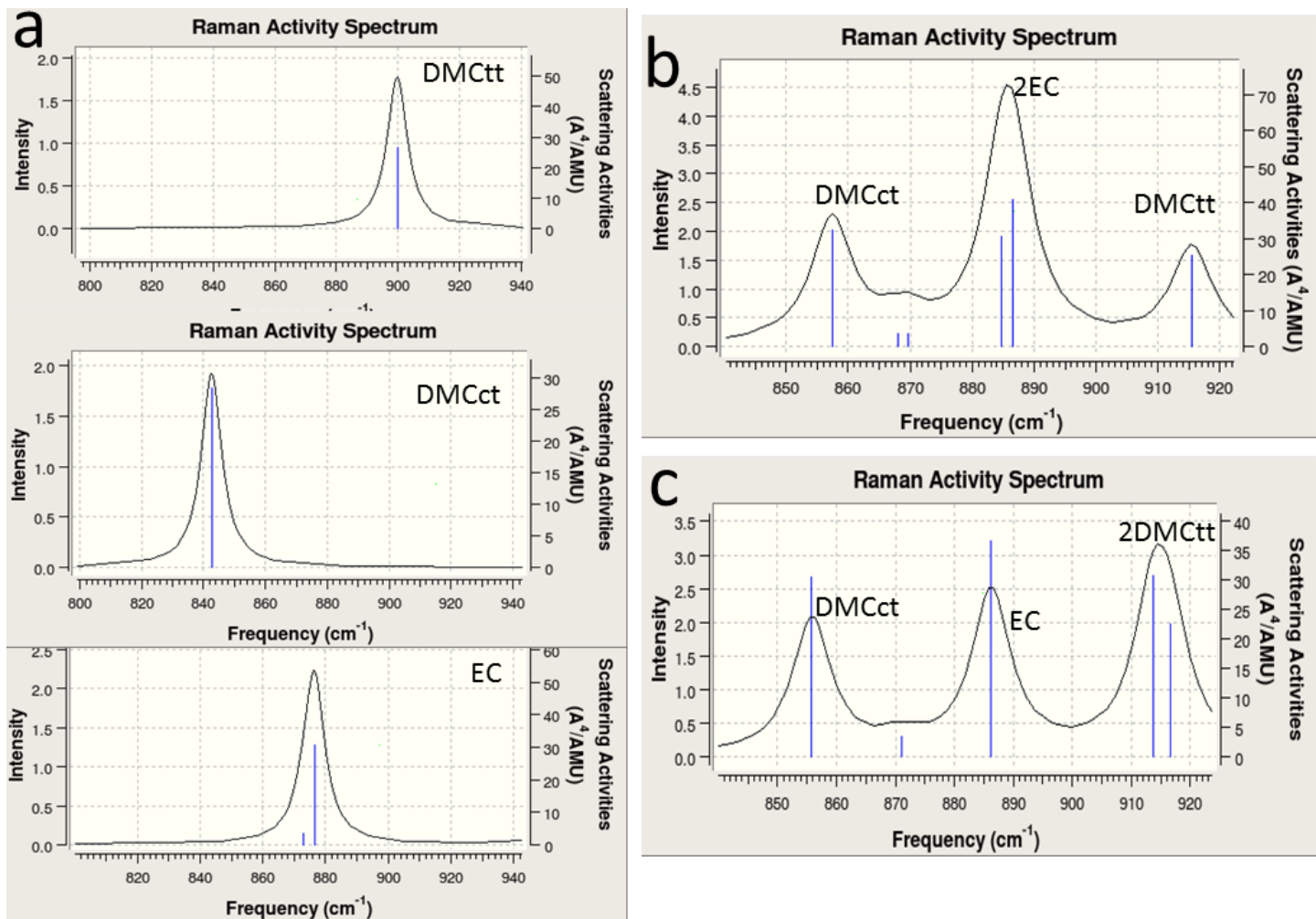


Fig. S9. Raman spectrum of isolated DMC and EC (a) and two Li⁺ solvates (b-c) from PBE/6-31+G(d,p) with SMD($\epsilon=20$, acetone) calculations.

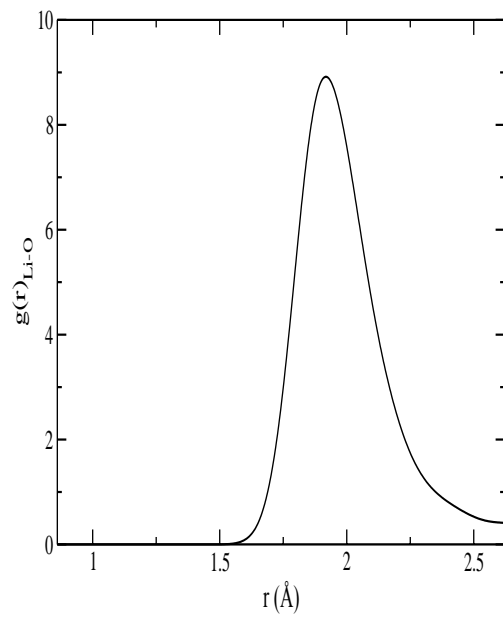


Fig. S10. (a) Radial distribution function $g(r)$ partial of Li-Carbonyl oxygen from our BOMD simulation of EC:DMC doped with one LiPF_6 at 400 K.

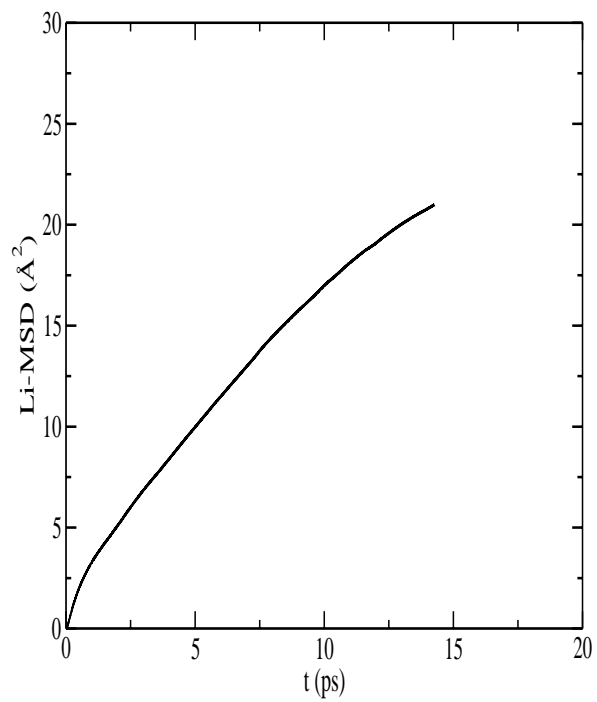


Fig. S11. The linear part of the MSD of EC:DMC doped with one LiPF_6 at 400 K.

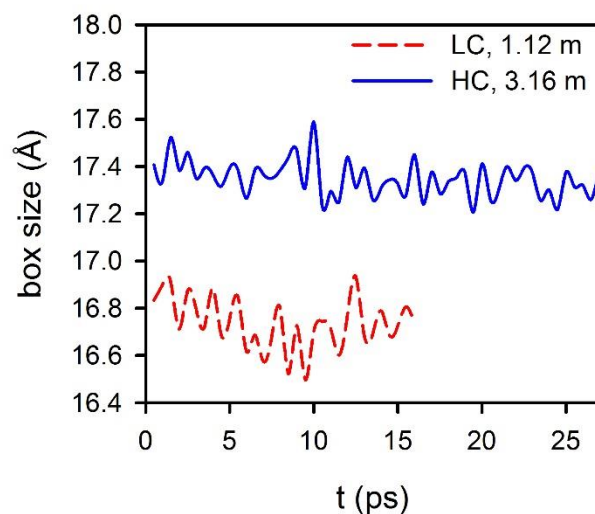


Fig. S12. The box size evolution during the NPT BOMD simulation run at 393 K using PBE functional. Note that first 4 ps of the LC run were omitted. While MD simulations showed a stable run on the scale of tens of ps, TGA experiments indicated a substantial weight loss at 393 K for 1 M LiPF₆ in EC:DEC electrolyte.³

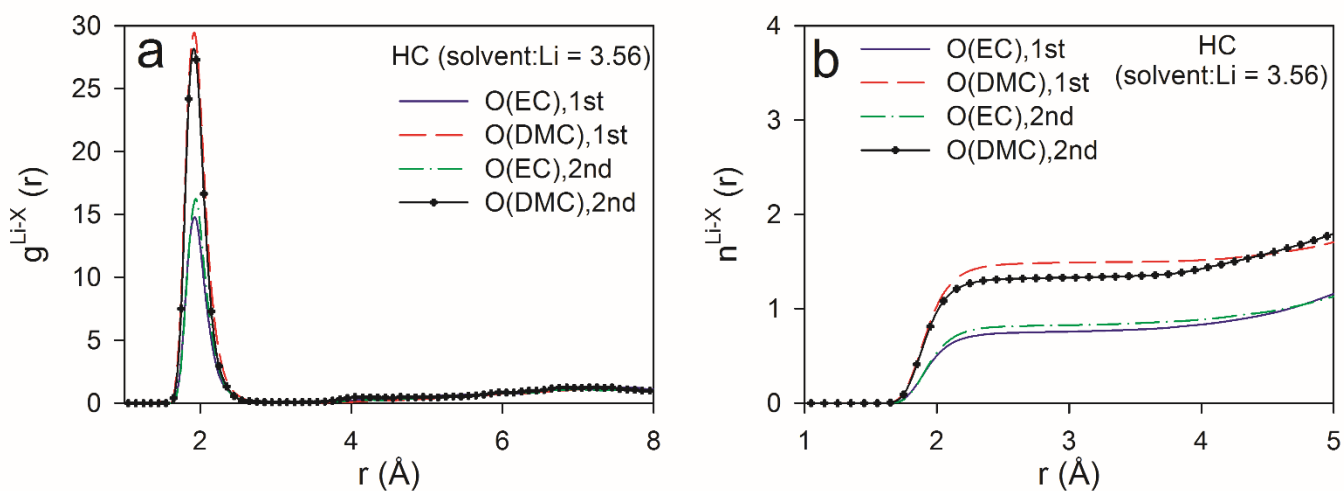


Fig. S13. Radial distribution functions ($g(r)$) and coordination numbers ($n(r)$) for HC EC:DMC/LiPF₆ electrolytes from BOMD simulations using PBE functional from the 1st and 2nd parts of the MD simulation trajectory. O denotes carbonyl oxygens.

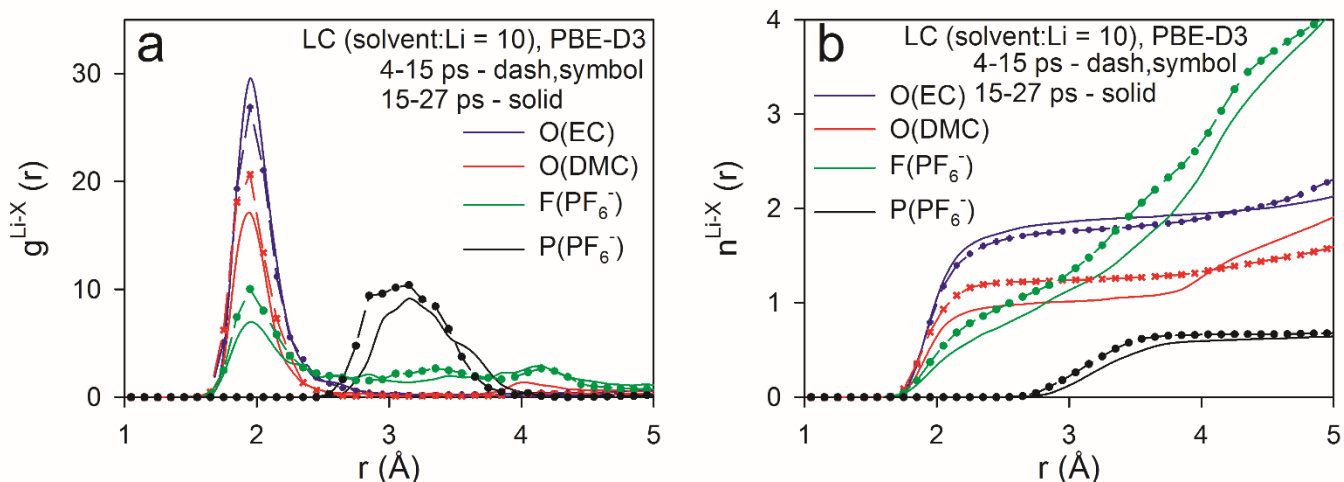


Fig. S14. Radial distribution functions ($g(r)$) and coordination numbers ($n(r)$) for LC EC:DMC/LiPF₆ electrolytes from BOMD simulations using PBE functional from the 1st and 2nd parts of the MD simulation trajectory.

O denotes carbonyl oxygen atoms.

Table S1. Binding energies relative to (EC)₄Li⁺ complex (in kcal/mol) from DFT calculations using a PBE functional with Grimme empirical dispersion corrections D2 and D3 or without them. The 6-31+G(d,p) basis set and SMD($\epsilon=20$, acetone) solvation model were employed.

	PBE	PBE-D2/PBE ^a	PBE-D3/PBE ^a
(EC) ₄ Li ⁺	0.0	0.0	0.0
(EC) ₃ (DMCcc)Li ⁺	0.4	-0.8	-1.1
(EC) ₂ (DMCcc)(DMCct)Li	1.4	-0.3	-0.9
(EC) ₂ (DMCcc) ₂ Li ⁺	0.5	-1.9	-2.5
EC(DMCcc) ₃ Li	1.2	-2.3	-3.3
(DMCct) ₃ (DMCcc)Li	3.6	1.0	0.1

^a PBE/6-31+G(d,p), SMD($\epsilon=20$, acetone) geometry was used for calculations with PBE-D2 and PBE-D3 density functionals.

References

1. J. Schmidt, J. VandeVondele, I. F. W. Kuo, D. Sebastiani, J. I. Siepmann, J. Hutter and C. J. Mundy, *Journal of Physical Chemistry B*, 2009, 113, 11959-11964.
2. G. J. Martyna, M. E. Tuckerman, D. J. Tobias and M. L. Klein, *Molecular Physics*, 1996, 87, 1117-1157.
3. D. W. McOwen, D. M. Seo, O. Borodin, J. Vatamanu, P. D. Boyle and W. A. Henderson, *Ener. & Env. Sci.*, 2014, 7, 416-426.